OPEN

Citation: Cell Death and Disease (2013) 4, e958; doi:10.1038/cddis.2013.490

www.nature.com/cddis

Placenta-derived mesenchymal stem cells improve memory dysfunction in an Aβ_{1-42}-infused mouse model of Alzheimer's disease

H-M Yun[1,6], HS Kim[2,3,6], K-R Park[1], JM Shin[2,3], AR Kang[2,3], K il Lee[2,3], S Song[1], Y-B Kim[4], SB Han[1], H-M Chung*[,5] and JT Hong*[,1]

Mesenchymal stem cells (MSCs) promote functional recoveries in pathological experimental models of central nervous system (CNS) and are currently being tested in clinical trials for neurological disorders, but preventive mechanisms of placenta-derived MSCs (PD-MSCs) for Alzheimer's disease are poorly understood. Herein, we investigated the inhibitory effect of PD-MSCs on neuronal cell death and memory impairment in Aβ_{1-42}-infused mice. After intracerebroventrical (ICV) infusion of Aβ_{1-42} for 14 days, the cognitive function was assessed by the Morris water maze test and passive avoidance test. Our results showed that the transplantation of PD-MSCs into Aβ_{1-42}-infused mice significantly improved cognitive impairment, and behavioral changes attenuated the expression of APP, BACE1, and Aβ, as well as the activity of β-secretase and γ-secretase. In addition, the activation of glia cells and the expression of inducible nitric oxide synthase (iNOS) and cyclooxygenase-2 (COX-2) were inhibited by the transplantation of PD-MSCs. Furthermore, we also found that PD-MSCs downregulated the release of inflammatory cytokines as well as prevented neuronal cell death and promoted neuronal cell differentiation from neuronal progenitor cells in Aβ_{1-42}-infused mice. These data indicate that PD-MSC mediates neuroprotection by regulating neuronal death, neurogenesis, glia cell activation in hippocampus, and altering cytokine expression, suggesting a close link between the therapeutic effects of MSCs and the damaged CNS in Alzheimer's disease.

Cell Death and Disease (2013) **4,** e958; doi:10.1038/cddis.2013.490; published online 12 December 2013
Subject Category: Neuroscience

Mesenchymal stem cell (MSC) has been recently considered to improve disease progression of neurological disorders.[1,2] MSC is a multipotent stem cell with capacity for self-renewal and differentiation with broad tissue distribution.[3] MSC was first identified and isolated from bone marrow (BM) more than 43 years ago.[4] However, within the bone marrow, BM-MSC is a rare cell population, resulting in a low MSC yield when isolated.[5] The progenitor pool may be depleted following extensive proliferation, leading to reducing ability to ensure regeneration after injury.[6,7] For these reasons, novel sources of MSCs are now being investigated for clinical use in diseases.[8,9] It was reported that MSCs derived from placenta (PD-MSCs) showed higher proliferative capacity and safety,[8,10] and also included noninvasive and ethically nonproblematic availability.[11] Thus, PD-MSCs can be obtained in large quantities, and the required numbers of these stem cells can be transplanted as an ideal alternative to adult bone marrow in therapeutic approaches for tissue replacement.

It was reported that BM-MSCs reduced Aβ levels in an acutely amyloid β (Aβ)-injected mouse model of Alzheimer's disease,[12] and attenuated Aβ-induced apoptotic cell death in primary cultured hippocampal neurons by the activation of the cell survival signaling pathway.[13] In amyloid precursor protein (APP) and PS1 double-transgenic mice, BM-MSCs significantly also reduced Aβ level associated with defective microglial function and decreased tau hyperphosphorylation and improved cognitive function.[14] Recently, human umbilical cord blood-(hUCB)-derived MSCs significantly also improved learning and memory decline through the modulation of neuroinflammation in an APP and PS1 double-transgenic mice.[15] Interestingly, no studies are available on the various roles played by PD-MSCs in eliciting the therapeutic effects in Alzheimer's diseases. Therefore, it is important to elucidate

[1]College of Pharmacy and Medical Research Center, Chungbuk National University, Cheongju, Chungbuk 361-763, Republic of Korea; [2]CHA Bio & Diostech Co., Ltd, 606-16 Yeoksam 1 dong, Gangnam gu, Seoul 135-970, Republic of Korea; [3]Department of Applied Bioscience, CHA University, Gyeonggi-do 463-836, Republic of Korea; [4]College of Veterinary Medicine, Chungbuk National University, Cheongju, Chungbuk 361-763, Republic of Korea and [5]Department of Stem Cell Biology, School of Medicine, Konkuk University, 120 Neungdong-ro Gwangjin-gu, Seoul 143-701, Republic of Korea
*Corresponding author: H-M Chung, Department of Stem Cell Biology, School of Medicine, Konkuk University, 120 Neungdong-ro, Gwangjin-gu, Seoul 143-701, Republic of Korea. Tel: +82 2 3468 3398; Fax: +82 2 3468 3373; E-mail: hmchung@cha.ac.kr
or JT Hong, College of Pharmacy and Medical Research Center, Chungbuk National University, 12 Gaeshin-dong, Heungduk-gu, Cheongju, Chungbuk 361-463, Republic of Korea. Tel: +82 43 261 2813; Fax: +82 43 268 2732; E-mail: jinthong@chungbuk.ac.kr
[6]These authors contributed equally to this work.
Keywords: PD-MSC; Alzheimer's disease; amyloid-β; cytokines; neurogenesis
Abbreviations: Aβ, amyloid β; APP, amyloid precursor protein; BM-MSC, bone marrow-derived MSC; β-secretase or BACE1, β-site APP cleaving enzyme 1; COX-2, cyclooxygenase-2; iNOS, inducible nitric oxide synthase; GCL, granule cell layer; MSC, mesenchymal stem cell; PD-MSC, placenta-derived MSC; SGZ, subgranular zone; UCB-MSC, umbilical cord blood-derived MSC
Received 24.7.13; revised 27.10.13; accepted 07.11.13; Edited by A Verkhratsky

the novel roles and potential effects mediated by PD-MSCs in Alzheimer's diseases.

Alzheimer's disease as one of the most important neurodegenerative disorders is an irreversible and progressive disorder with observable memory impairment.[16,17] Aβ is generated from APP, a membrane-spanning protein to be digested by β-secretase (β-site APP cleaving enzyme 1 (BACE1)).[18,19] It was reported that APP metabolism and Aβ generation associated with senile plaques are related to the activation of glia cells.[20] Aβ peptide activates glia cells that are found to surround Aβ plaques.[21,22] The activation of these cells is associated with many inflammation-associated neurodegenerative diseases including Alzheimer's disease.[23,24] It is also suggested that glia cells could act as a source for Aβ because they overexpress BACE1 in response to chronic stress.[25] Thus, the feed-forward vicious cycle by Aβ between amyloidogenesis and neuroinflammation culminates in widespread neuronal dysfunction and cell death, leading to progressive Alzheimer's disease associated with extensive Aβ pathology.

In the present study, we examined whether the transplantation of PD-MSCs could have beneficial effects in Aβ_{1-42}-infused mice model. We found that the transplantation of PD-MSCs rescued cognitive impairment, promoted antiamyloidogenic and anti-inflammatory response, and also increased neuronal survival and neurogenesis.

Results

PD-MSC reverses memory impairment in Aβ_{1-42}-infused mice. In order to identify whether PD-MSCs could affect memory impairment by Aβ_{1-42} in Alzheimer's diseases, ICR mice were infused with Aβ_{1-42} (300 pmol per day per mouse) for 14 days and then compared memory deficiency between the control mice and mice transplanted with PD-MSCs (1×10^5, 5×10^5, and 1×10^6 cells per mouse) via intravenous injection into mouse tail vein. As shown in Figure 1, we performed behavioral tests for a total of 12 days using the Morris water maze and passive avoidance tests. All mice were trained for three trials per day for 7 days. Escape latency (time, s) and swimming distance (distance, cm) that were traveled to reach a platform in water maze were measured to determine memory impairment effect of PD-MSCs. The Aβ_{1-42}-infused mice exhibited significantly delayed escape latency (33.2 ± 17.94 s, $^{**}P<0.01$; Figure 2a) and swimming distance (851.5 ± 123.5 cm, $^{**}P<0.01$; Figure 2b) compared with the control mice (escape latency: 17.2 ± 10.03 s; swimming distance: 418.2 ± 75.21 cm); however, mice transplanted with PD-MSCs showed significantly better performance on the water maze test than Aβ_{1-42}-infused mice (1×10^5 cells: 25.5 ± 12.68 s, 583.3 ± 152.8 cm, $^{\#\#}P<0.01$; 5×10^5 cells: 28.4 ± 14.38 s, 541.3 ± 138.3 cm, $^{\#\#}P<0.01$; 1×10^6 cells: 22 ± 6.60 s, 489.3 ± 61.02 cm, $^{\#\#}P<0.01$; Figures 2a and b).

After the water maze test, a probe test was performed in which the platform was removed to analyze whether the animals used a nonspatial strategy to find the platform. During the probe test, we calculated the time spent in the target quadrant zone during the 60 s test. The memory deficiency in Aβ_{1-42}-infused mice (15.92 ± 10.32 s, $^{*}P<0.05$) was significantly improved in PD-MSC mice group (1×10^5 cells: $25.89\pm7.51\%$; 5×10^5 cells: $28.58\pm7.63\%$, $^{\#}P<0.05$; 1×10^6 cells: $30.84\pm5.27\%$, $^{\#}P<0.05$; Figure 2c). To determine whether PD-MSC mice improved the contextual memory in Aβ_{1-42}-infused mice, we next evaluated learning and memory capacities by the passive avoidance test using the step-through method. In the passive avoidance test, there was no significant difference on the learning trial. In contrast, PD-MSC mice (1×10^5 cells: 31.58 ± 7.67 s, $^{\#}P<0.05$; 5×10^5 cells: 39.45 ± 8.19 s, $^{\#\#}P<0.01$; 1×10^6 cells: 41.13 ± 10.27 s, $^{\#\#}P<0.01$) significantly increased the step-through latency compared with the Aβ_{1-42}-infused mice (20.23 ± 6.54 s, $^{***}P<0.001$; Figure 2d). Thus, we validated that the beneficial effects of PD-MSCs remained consistent over a prolonged period of time. These results indicate that PD-MSC improves deficits of learning and memory in Aβ_{1-42}-infused mice.

PD-MSC reveals antiamyloidogenic effects in Aβ_{1-42}-infused mice. We investigated whether PD-MSCs influenced amyloidogenesis in the Aβ_{1-42}-infused mice. The number of Aβ_{1-42}-reactive cells was determined with immunohistochemical analysis and Aβ_{1-42} expression was significantly lowered by the transplantation of PD-MSCs (Figure 3a) and the levels of Aβ_{1-42} were also measured using ELISA (Con: 13.00 ± 8.06; Aβ: 33.53 ± 5.44, $^{*}P<0.05$; A$\beta+$MSC: 19.79 ± 4.01, $^{\#}P<0.05$; Figure 3e). To clarify how Aβ_{1-42} deposition had occurred, we analyzed the expression level of APP and BACE1. As shown in Figures 3b–d, there was a significant rise in the level of the proteins in the brain after Aβ_{1-42} injection, which was inhibited by PD-MSCs. To confirm the speculation, we next attempted to measure β- and γ-secretase activity. The activity of β- and γ-secretase significantly increased in the brain of Aβ_{1-42}-infused mice (β-secretase: Aβ, 420.5 ± 39.77, $^{*}P<0.05$; γ-secretase: Aβ, 245.2 ± 14.15, $^{**}P<0.01$), whereas the alteration in β- and γ-secretase activity was attenuated by the transplantation of PD-MSC (β-secretase: A$\beta+$MSC, 348.0 ± 7.45, $^{\#}P<0.05$; γ-secretase: A$\beta+$MSC, 141.3 ± 20.71, $^{\#\#}P<0.01$; Figures 3f and g). These data suggest that PD-MSC has an antiamyloidogenic effect in Aβ_{1-42}-infused mice.

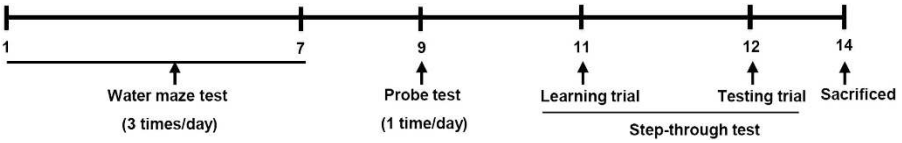

Figure 1 The scheme of experimental study on an Aβ_{1-42}-infused mouse model. After Aβ infusion for 14 days, the Morris water maze test, probe test, and passive avoidance test were conducted as shown

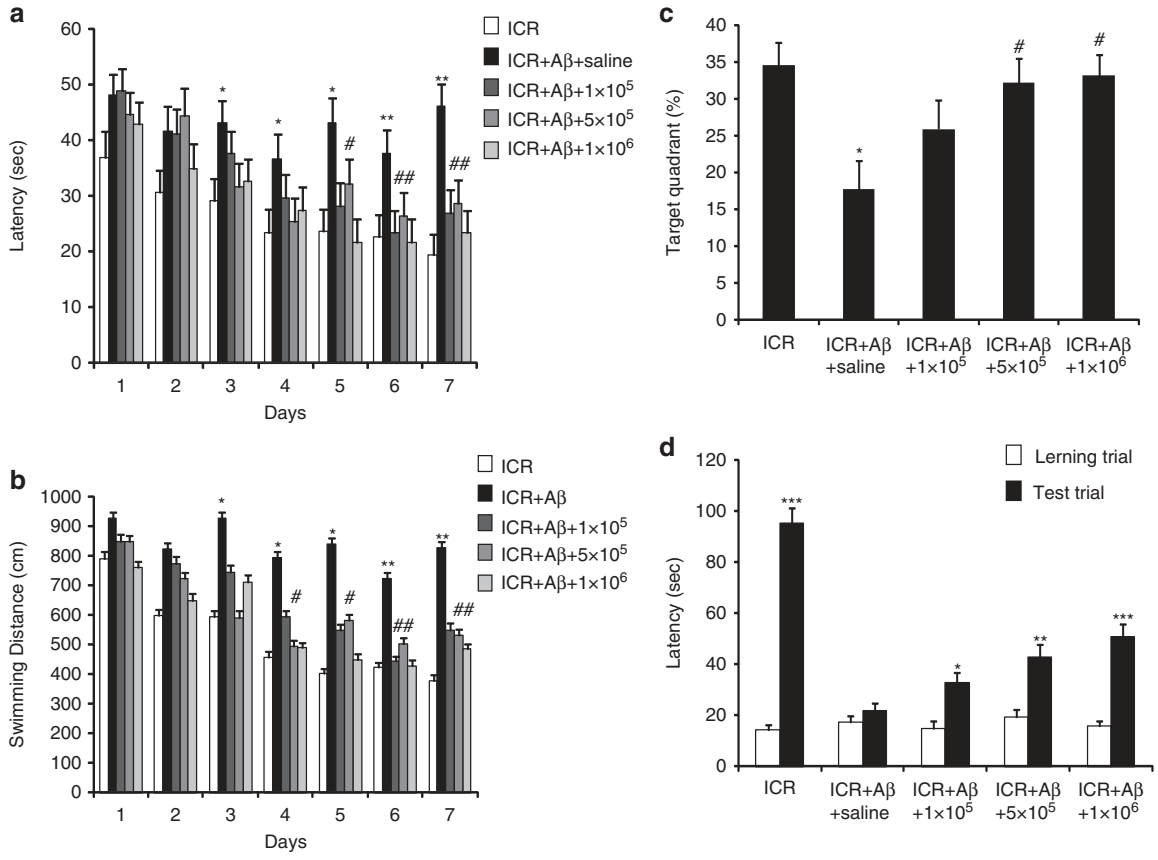

Figure 2 Inhibitory effects of PD-MSCs on memory impairment in Aβ_{1-42}-infused mice model. (**a**–**c**) Training trial was performed three times a day for 7 days. Swimming time (**a**) and swimming distance (**b**) to arrive at platform were automatically recorded. At 24 h after training trials, a probe test was performed. The time spent in the target quadrant and target site crossing within 60 s was represented (**c**). Each value is presented as mean ± S.E.M. from 10 mice. (**d**) To perform passive avoidance test, the mice were given electric shock when entered into the dark compartment for training on learning day. After 1 day, the retention time in illuminated compartment was recorded. Each value is presented as mean ± S.E.M. from 10 mice. Significant difference from control mice (*$P<0.05$, **$P<0.01$, and ***$P<0.001$). Significant difference from Aβ_{1-42}-infused mice ($^{\#}P<0.05$ and $^{\#\#}P<0.01$)

PD-MSC reveals antineuroinflammatory effects in A$\beta\beta_{1-42}$-infused mice. It was also reported that activation of glia cells is one of the characteristic feature in the Alzheimer's disease, and they can produce inflammatory cytokines as well as generate Aβ when they are activated. Therefore, we compared activation of astrocytes and microglia in the brains between Aβ_{1-42}-infused mice and Aβ_{1-42}-infused PD-MSC mice. As shown in Figures 4a and b, GFAP-positive cell numbers (astrocytes) and Iba1-positive cell number (microglia) were much higher in the brains of Aβ_{1-42}-infused mice as compared with the brains of Aβ_{1-42}-infused PD-MSC mice. To verify these results, we investigated the expression of GFAP and Iba1 by western blotting. The results revealed that the GFAP and Iba1 levels were significantly increased in Aβ_{1-42}-infused mice as compared with control mice. However, Aβ_{1-42}-infused PD-MSC mice were significantly attenuated the expression of GFAP and Iba1 in the Aβ_{1-42}-infused mice (Figure 4e). We also demonstrated the effect of the transplantation of PD-MSCs on memory formation and Aβ deposition was mediated by neuroinflammation. The expression of the inflammatory protein such as inducible nitric oxide synthase (iNOS) and cyclooxygenase-2 (COX-2) in the brain of Aβ_{1-42}-infused mice were significantly increased than the control mice, whereas PD-MSC mice revealed a decrease in the expression of iNOS and COX-2 detected by immunohistochemical analysis (Figures 4c and d) and western blotting (Figure 4e). To validate the activation of glia cells and inflammatory response, we performed mouse cytokine array using Proteome profiler arrays. We found that the levels of G-CSF, I-309, sICAM-1, IFN-γ, IL-1β, IL-7, IL-17, IL-27, IP-10, KC, MIG, CCL5, TIMP-1, and TNF-α by infusion of Aβ_{1-42} were significantly altered, which is inhibited by PD-MSC (Supplementary Figure 1). Our results indicate that PD-MSC regulates glia cells, inflammatory response, and cytokine release to improve the symptom in Alzheimer's diseases.

PD-MSC prevents neuronal cell death and promotes neuronal differentiation. We explored whether PD-MSC was able to improve memory impairment by preventing Aβ_{1-42}-induced neuronal cell death. In the CA1, CA3, and dentate gyrus (DG) region of the hippocampus, Aβ_{1-42} injection significantly increased apoptotic cell death as compared with control mice (CA1: 88.69 ± 9.30, $P<0.001$; CA3: 78.64 ± 9.35, $P<0.01$; DG: 68.81 ± 13.05, $P<0.05$). PD-MSCs inhibited apoptotic cell death in Aβ_{1-42}-infused

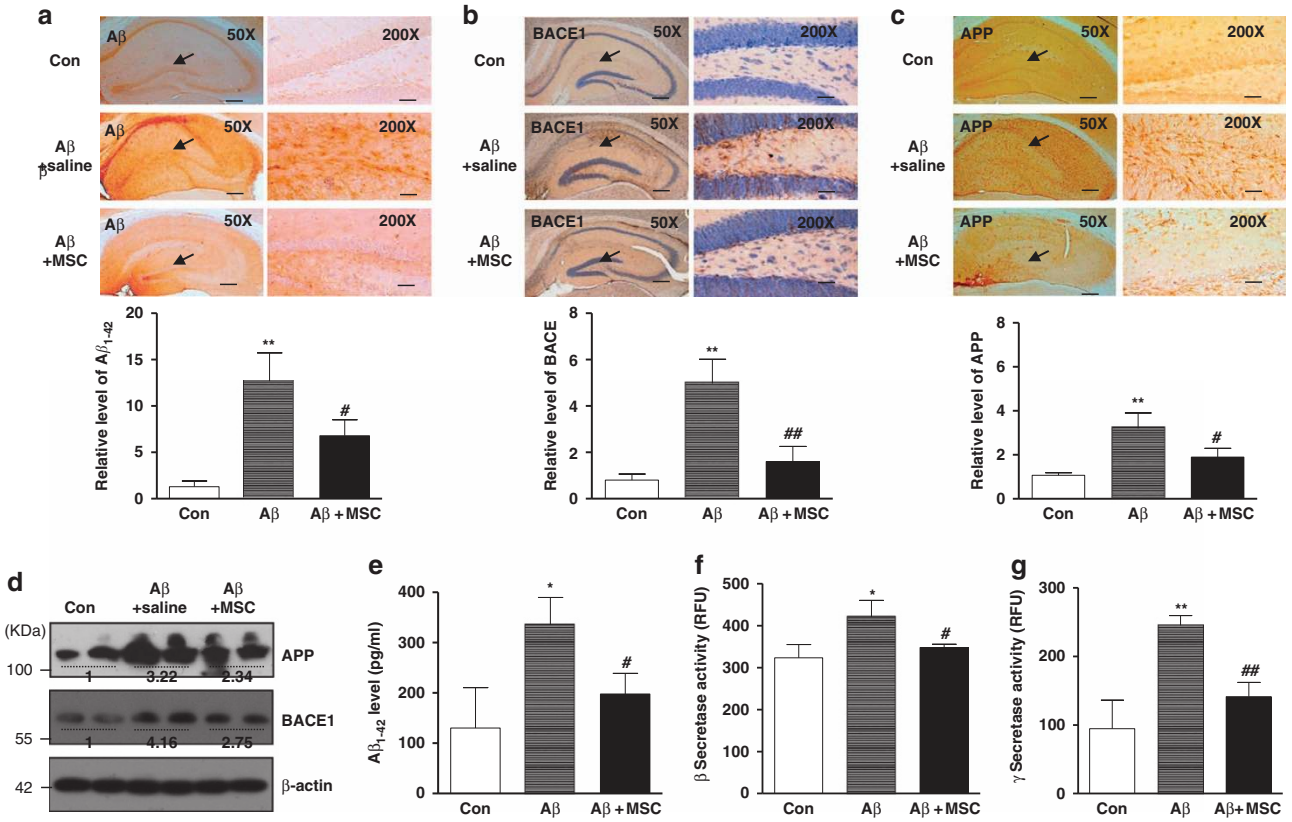

Figure 3 Inhibitory effects of PD-MSCs on Aβ_{1-42}, BACE1 and APP in the brain of Aβ_{1-42}-infused mice. (**a–c**) Aβ_{1-42}, BACE1, and APP were observed by immunohistochemical analysis as described in the Materials and Methods. The sections of brains were incubated with anti-Aβ_{1-42} (**a**), anti-BACE1 (**b**), and anti-APP (**c**) antibodies, followed by biotinylated secondary antibody. Immunoperoxidase staining was expressed as brown color. (**d**) The expression of APP and BACE1 were detected by western blotting using specific antibodies in brain lysates. β-Actin was used as an loading control. (**e**) Aβ_{1-42} level was measured in mouse brains by ELISA as described in the Materials and Methods. Value is mean ± S.E.M. of 8 mice. (**f** and **g**) The activities of β-secretase (**f**) and γ-secretase (**g**) were carried out using each assay kit as described in the Materials and Methods. Values measured from each group of mice were calibrated by amount of protein and expressed as mean ± S.E.M. from 8 mice. Significant difference from control mice ($^{*}P<0.05$ and $^{**}P<0.01$). Significant difference from Aβ_{1-42}-infused mice ($^{\#}P<0.05$ and $^{\#\#}P<0.01$). The experiments shown in Figure 2 were repeated in triplicate with similar results

mice (CA1: 48.56 ± 5.21, $P<0.05$; CA3: 43.23 ± 10.61, $P<0.05$; DG: 31.56 ± 4.80, $P<0.05$; Figures 5a–d). Moreover, we investigated whether Aβ_{1-42} infusion or PD-MSC affects neuronal precursor cells to be differentiated into neuron. As shown in Figure 5e, in the subgranular zone (SGZ)–granule cell layer (GCL) of the hippocampus, Aβ_{1-42}-infused mice revealed that DCX-positive cells (adult–newborn neurons) were diminished when compared with control mice, whereas the implantation of PD-MSC recovered adult–newborn neurons decreased by Aβ. Ki-67-positive cells were not changed between control, Aβ_{1-42}-infused, and PD-MSC mice (Figure 5f), implying that PD-MSCs did not affect proliferation of adult neural stem cell. As MSC is a multipotent cell that can be differentiated into neural cell lineages, we therefore investigated whether the protective effects of PD-MSCs were mediated by direct differentiation into neuron or glia cells. As shown in Figure 6, PD-MSCs implanted in Aβ_{1-42}-infused mice was not colocalized with NeuN (mature neuron) (Figure 6a), DCX (newborn neuron; Figure 6b), or GFAP (astrocyte; Figure 6c) positive cells. Taken together, these data suggest that PD-MSC prevents neuronal cell death and induces newly generated neuron regardless of the neural differentiation potential of PD-MSC.

Discussion

In the present study, we originally reported clear evidences in the role of PD-MSCs using an Aβ-infused mouse model of Alzheimer's diseases. Aβ-infused mouse model has been used to directly investigate the toxicity of Aβ that consisted of senile plaques of Alzheimer's disease.[12,13,26–28] Also, we continually investigated amyloidogenesis, neuroinflammation, and memory impairment through the injection of Aβ.[29–33] Therefore, to investigate the effect on the Aβ toxicity of PD-MSCs, we used the Aβ-infused mouse model in the present study. We demonstrated that the transplantation of PD-MSCs in Aβ_{1-42}-infused mice has antiamyloidogenic and antineuroinflammatory effects to improve neuronal survival and neurogenesis, and prevent memory deficiency.

Amyloidogenesis postulates that gradual changes in the metabolism and aggregation of Aβ initiate a cascade of neuronal and inflammatory injury that culminates in extensive neuronal dysfunction and cell death in Alzheimer's disease.[34,35] In these experiments, we demonstrated that PD-MSCs reduced the amyloid cascade in the Aβ_{1-42}-infused mouse model. The effect of PD-MSC is likely attributable to inhibition in the expression of BACE1 and APP, and the

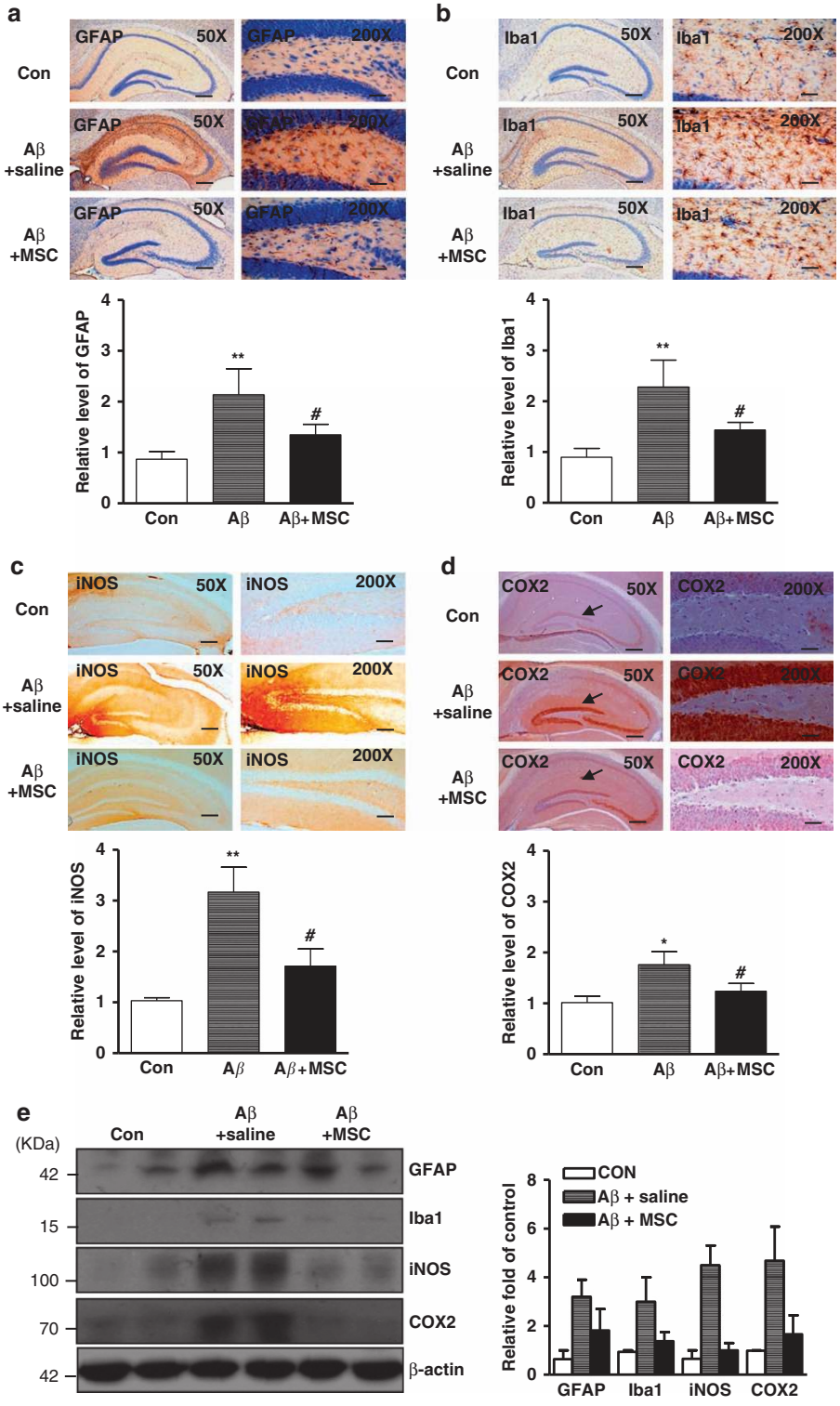

Figure 4 PD-MSC inhibits the activation of astrocytes and microglia, and reduces the expression of COX-2 and iNOS. (**a** and **b**) The effect of PD-MSC on reactive astrocytes and activated microglia cells was measured by immunohistochemical analysis. The sections were incubated with antiglial fibrillary acidic protein (GFAP) (**a**) and anti-ionized calcium binding adaptor molecule 1 (Iba1) (**b**) antibodies, followed by the biotinylated secondary antibody ($n=8$). Immunoperoxidase staining was expressed as brown color. (**c** and **d**) The sections were incubated with anti-iNOS (**c**) and anti-COX-2 (**d**) antibodies, and then followed by the biotinylated secondary antibody ($n=8$). Immunoperoxidase staining was expressed as brown color. (**e**) The expression of GFAP, Iba1, iNOS, and COX-2 was detected by western blotting using specific antibodies. The signals of GFAP, Iba1, iNOS, and COX2 were normalized using β-actin and the numerical values were expressed as relative fold of control. Significant difference from control mice ($^{*}P<0.05$ and $^{**}P<0.01$). Significant difference from $A\beta_{1-42}$-infused mice ($^{\#}P<0.05$). The experiments shown in Figure 3 were repeated in triplicate with similar results

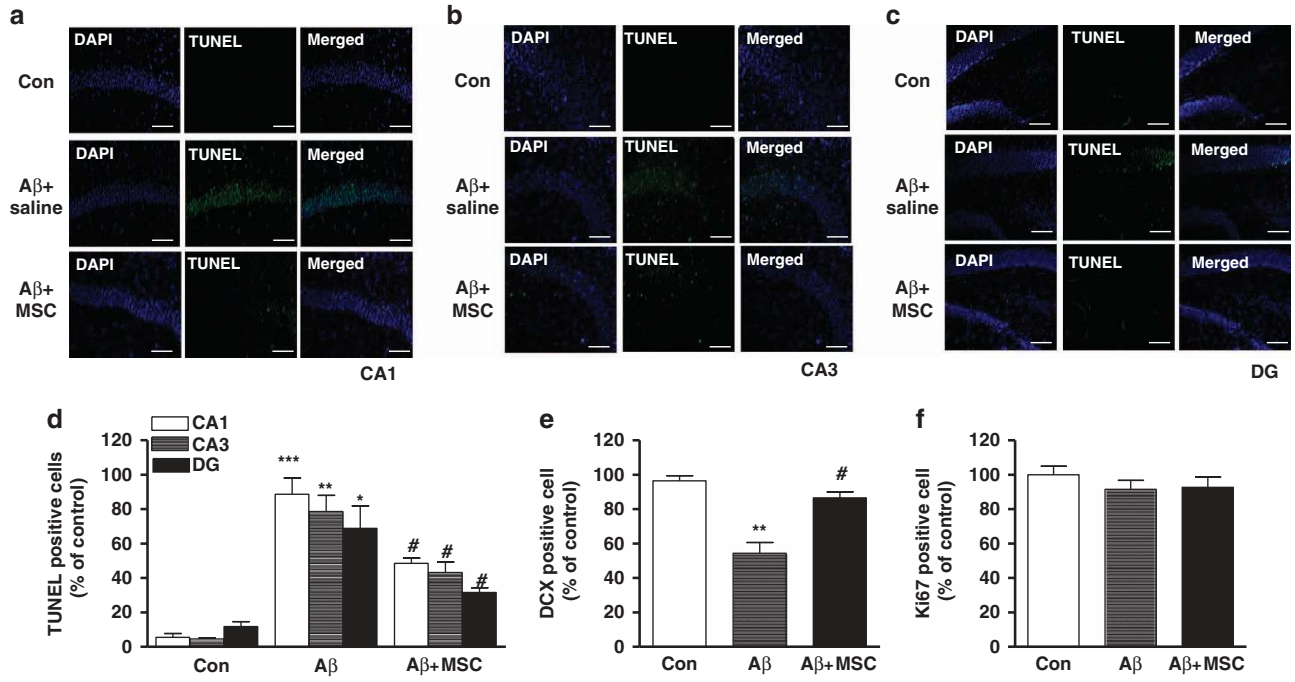

Figure 5 PD-MSC prevents Aβ_{1-42}-induced apoptotic cell death and promotes neuronal differentiation. (**a**–**c**) Representative photographs (original magnification $\times$ 100) of each region of control mice, Aβ_{1-42}-infused mice, and PD-MSC (1×10^6 cells) mice. Apoptotic cell death in hippocampus CA1 (**a**), CA3 (**b**), and DG (**c**) of mouse brain was determined by DAPI and TUNEL staining as described in the Materials and Methods. (**d**) DAPI- and TUNEL-positive cells were counted in three separate locations and expressed as % of control. Significant difference from control mice ($^*P<0.05$, $^{**}P<0.01$, and $^{***}P<0.001$). Significant difference from Aβ_{1-42}-infused mice ($^{\#}P<0.05$). (**e** and **f**) The effect of PD-MSC on newly generated neurons and proliferation of neural stem cells was measured by immunohistochemical analysis. The sections were incubated with anti-doublecortin (DCX) (**e**) and anti-antigen Ki-67 (Ki-67) (**f**) antibodies, followed by the biotinylated secondary antibody ($n=8$). Significant difference from control mice ($^{**}P<0.01$). Significant difference from Aβ_{1-42}-infused mice ($^{\#}P<0.05$). The experiments shown in Figure 4 were repeated in triplicate with similar results

activity of γ-secretase. Amyloidogenic processing of APP involves sequential cleavages by BACE1 and γ-secretase.[35] C-terminal fragment of APP generated by BACE1 cleavage was further processed by γ-secretase to produce A$\beta_{40/42}$. Our results indicated that the expression of BACE1 and APP, and the activity of γ-secretase, were decreased by PD-MSCs in Aβ_{1-42}-infused mice. Previously, it was reported that BM-MSCs significantly reduced Aβ deposition and attenuated Aβ-induced memory impairment and apoptosis by inhibiting neuronal cell death.[12–14] Adipose tissue-derived MSCs also improved cognitive function in aging mice.[36] Thus, we suggest that PD-MSC improves cognitive dysfunction through BACE1 and APP expression, and γ-secretase activities to diminish amyloidogenesis.

APP and BACE1 are upregulated in astrocytes and microglia upon exposure to cytokines influencing APP processing to induce amyloidogenesis, and induced in the proximity of activated astrocytes and microglia.[37,38] We found that the number of astrocytes and microglia were elevated in Aβ_{1-42}-infused mice that were prevented by PD-MSCs. It was also reported that BACE1 and APP transcriptions are increased by other inflammatory gene expression such as iNOS and COX-2.[39,40] Several studies have indicated that neuroinflammatory reactions could contribute to BACE1 and APP expression and γ-secretase activity. These studies also support the idea for neuroinflammation as a direct effect on amyloidogenesis. Especially, hUCB-derived MSCs significantly reduced the levels of Aβ, BACE1, and Tau hyperphosphorylation by regulating neuroinflammatory responses including alternatively elevated microglia and decreased proinflammatory cytokines (IL-1β and TNFα).[15] In present study, we also found that PD-MSCs inhibited neuroinflammatory responses through decreased iNOS and COX-2 expression, decreased proinflammatory cytokines including IL-1β and TNFα, and inactivated glia cells. These results suggest that the inhibitory effect of PD-MSCs on the activation of astrocytes and microglia might be significant to modulate neuroinflammatory-mediated amyloidogenesis. Based on previous reports in Alzheimer's diseases patients and animal models,[41–43] we speculated whether activated microglia and astrocytes by Aβ also caused cytokine releases. As a result of mouse cytokine array, the transplantation of PD-MSCs also inhibited cytokine secretion induced in Aβ_{1-42}-infused mice. We found that the levels of cytokines including IL-1β, IL-17, TNF-α, and IP-100 were significantly altered by Aβ_{1-42} that were inhibited by PD-MSCs. IL-1β, IL-17, and TNFα have important roles in affected brain regions in association with plaques and tangles in Alzheimer's disease.[44,45] Aβ induces the production and secretion of IL-1β,[46] and astrocytes induce neuronal death by induction of IL-1β and IL-17, together with TNFα.[47] TNFα binds to neuronal Cd120a/b receptors triggering caspase activation through death effector domains.[48] IP-10 is markedly increased in reactive astrocytes in Alzheimer's disease brains, and IP-10-positive astrocytes are associated with senile plaques and Aβ-induced neurotoxicity.[49,50] Similar to our observation,

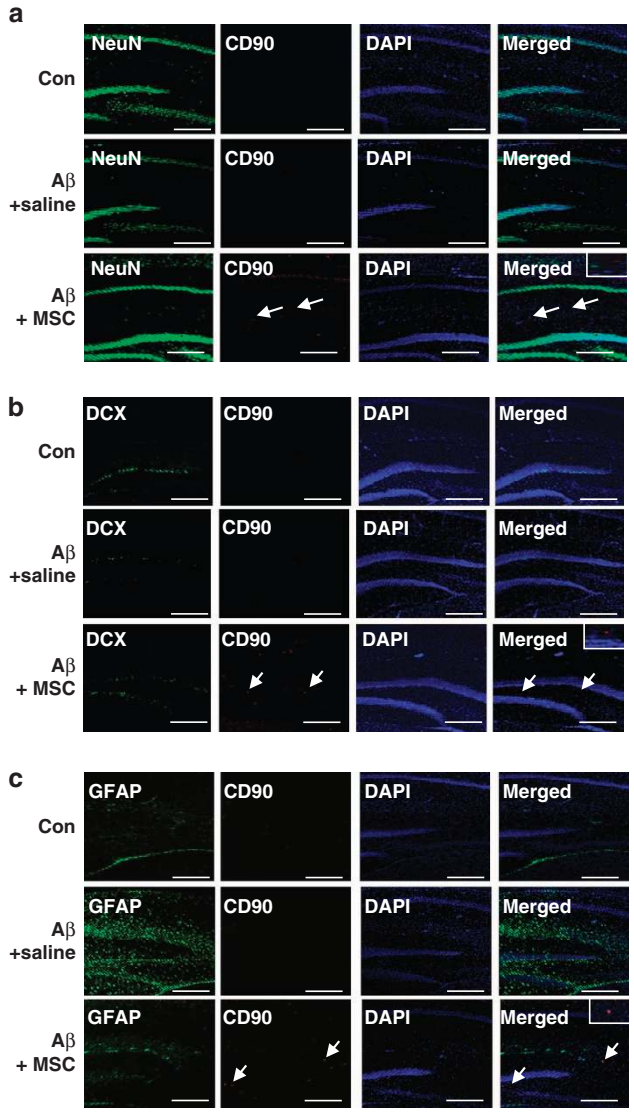

Figure 6 The localization of PD-MSCs with NeuN, DCX, and GFAP in Aβ_{1-42}-infused mice. (**a**–**c**) Immunofluorescence analysis using confocal microscope in Aβ_{1-42}-infused mice. The sections were fixed and permeabilized. Mature neuron (**a**), newborn neuron (**b**), and astrocytes (**c**) (green, left) were immunostained with anti-NeuN, anti-DCX, and anti-GFAP antibodies, and then followed by Alexa488-conjugated secondary antibodies. PD-MSC (red, middle) was immunostained with anti-CD90 antibody, and then followed by Alexa555-conjugated secondary antibodies. The right panels of (**a**–**c**) show the merged images of the left and middle panels. The experiments shown in Figure 5 were repeated in triplicate with similar results

MSC tends to be migrated and localized to tissues that undergo an inflammatory response, altering the spectrum of local cytokines.[51] MSC is a multipotent cell that can be differentiated into a variety of cell types, including: osteogenic, chondrogenic, adipogenic, and neural cell lineages.[52] However, in the mouse brain, PD-MSC was not differentiated into neural cell. Therefore, our results implied that PD-MSCs might have a role in the memory improvement in Alzheimer's diseases because of the antineuroinflammatory reaction-associated antiamyloidogenesis, but not the multipotency of PD-MSCs.

Inflammation is also frequently associated with hippocampal neurogenesis that causes deficits in cognition.[53] The cognitive deficits associated with Alzheimer's diseases were ameliorated by stimulation of cell proliferation and survival and integration of newborn cells into neuronal network of the SGZ–GCL of the hippocampus.[54] The decrease of hippocampal neurogenesis is associated with behavioral deficits and developed with age, in parallel with the development of Alzheimer's diseases.[55,56] Neural stem cells in the hippocampus are located in the SGZ at the border between the GCL and hilus of the DG.[57] Some of the daughter cells produced by division of those precursor cells differentiate into neurons and develop the prominent apical dendrite that characterizes dentate granule neurons as they move into the GCL.[58] Adult–newborn neurons (DCX-positive cells) project axons to the primary target of dentate granule neurons and the stratum lucidum of CA3 area, and then integrated into the hippocampal circuitry.[59] In Aβ_{1-42}-infused mice model, a decrease in hippocampal neurogenesis was detected on the SGZ at the border between the GCL and hilus of the DG, whereas PD-MSCs recovered neurogenesis of adult neural progenitor cells. Overall, our data indicated that PD-MSCs could also improve memory function through partially enhanced neurogenesis.

In conclusion, our data not only provide novel evidences of PD-MSCs on inflammation-mediated amyloidogenesis, neurogenesis, and neuroprotection in an Aβ_{1-42} infused mice model, but also our findings strongly support the therapeutic potential and clinical use of PD-MSCs in Alzheimer's diseases.

Materials and Methods

Animals. Male ICR mice (20–25 g) were purchased from Samtako (Seoul, Korea) and were maintained in accordance with the National Institute of Toxicological Research of the Korea Food and Drug Administration guideline for the humane care and use of laboratory animals. All experimental procedures in the present study were approved by the IACUC of Chungbuk National University (approval number: CBNUA-144-1001-01). Animals were housed in a room that was automatically maintained at 21–25°C and relative humidity (45–65%) with a controlled light–dark cycle. All animals had free access to food (Samyang Foods, Seoul, Korea) and water.

Isolation and expansion of human PD-MSCs. Normal human placentas with no evidence of medical, obstetrical, or surgical complications were collected from normal full-term pregnancies ($\geq$37 weeks of gestational age). All donors provided written informed consent before placenta collection. The protocols for sample isolation and their subsequent use for research purposes were approved by the institutional review board (IRB) of the Bundang CHA General Hospital, Korea. PD-MSC was harvested from the amniochorionic membrane of placentas obtained after Cesarean section. We isolated PD-MSCs and characterized them (Supplementary Figure 2) as previously described.[60] Briefly, the chorioamniotic membrane was peeled and separated from the placenta. Subsequently, the amnion and innermost membrane from the chorion and decidua were removed. These tissues were washed several times in phosphate-buffered saline (PBS, Gibco, Grand Island, NY, USA), and then cells of chorionic plate side scraped from the membrane were removed and the remainder membrane was dissected and minced in a Petri dish. The minced tissue was transferred to a 50 ml centrifuge tube and digested for 30 min at 37°C shaking incubator containing Hank's balanced salt solution (HBSS, Gibco) with a combination of 2 mg/ml trypsin (Sigma, St. Louis MO, USA), 20 μg/ml DNaseI (Sigma), 1.2 U/ml Dispase (Gibco), and 1 mg/ml Collagenase type IV (Sigma). The harvested cells were cultured in T25 flasks (BD Biosciences, San Jose, CA, USA) in MEM-α GlutaMAX supplemented with 10% fetal bovine serum (Gibco) and 25 ng/ml FGF4 (R&D System, Minneapolis, MN, USA), and 1 μg/ml heparin (Sigma) at 37°C in an

atmosphere of 5% CO_2 and 3% O_2. When cells reached 70–80% confluence, adherent cells were dissociated with TrypLE (Gibco), washed, and replated at a concentration of 4×10^3 cells/cm^2.

Aβ_{1-42}-infused mouse model. The infusion mouse model was adapted from previous work on the rat infusion model (Nitta *et al.*[26]). The anesthetized animals were placed in a sterotaxic instrument and catheters were attached to an osmotic mini-pump (Alzet 1002, ALZA, Mountain View, CA, USA) and brain infusion kit 1 (Alzet kit 3–5 mm, ALZA) that were implanted according to the following coordinates: mouse (unilaterally): -1.0 mm anterior/posterior, $+0.5$ mm medial/lateral, and -2.5 mm dorsal/ventral. The pump contents were released over a period of 14 days consisting of 300 pmol aggregated Aβ_{1-42} (Bachem Chemical, Torrance, CA, USA) dissolved in sterile saline (0.9% NaCl) for each pump.

Water maze test. The learning and memory capacity was assessed using two separate tests (water maze and passive avoidance test). The water maze test is a widely accepted method for testing memory. The examination was performed using the SMART-CS (Panlab, Barcelona, Spain) program and equipment. A circular plastic pool (height 35 cm, diameter 100 cm) was filled with water (containing milk) kept at 22–25°C. An escape platform (height 14.5 cm, diameter 4.5 cm) was positioned submerged 0.5–1 cm below the surface of the water. The test was performed three times per day for 7 days. Each trial lasted for 60 s or ended as soon as the mouse reached the submerged platform and was allowed to remain on the platform for 2 s. The mice were allowed to swim until they sought the escape platform. Escape latency, escape distance, swimming speed, and swimming pattern of each mouse were monitored by a camera above the center of the pool connected to a SMART-LD program (Panlab). A quiet environment, consistent lighting, constant water temperature, and fixed spatial frame were maintained throughout the period of the experiment.

Probe test. A probe test to assess memory consolidation was performed 2 days after the 7-day acquisition tests. In this test, the platform was removed from the tank, and the mice were allowed to swim freely. For these tests, the spent time on the target quadrant within 60 s was recorded. The time spent in the target quadrant was taken to indicate the degree of memory consolidation that had taken place after learning. The swimming pattern of each mouse was monitored by a camera above the center of the pool connected to a SMART-LD program as described above.

Passive avoidance performance test. The passive avoidance test is also widely accepted as a simple and rapid method for testing memory. The passive avoidance response was determined using a 'step-through' apparatus (Med Associates, Georgia, VT, USA) that consists of an illuminated and a dark compartment (each $20.3 \times 15.9 \times 21.3$ cm) adjoining each other through a small gate with a grid floor of 3.175 mm stainless steel rods set 8 mm apart. At 1 day after the probe test, the training trial was performed. The mouse was placed in the illuminated compartment facing away from the dark compartment. When the mouse moved completely into the dark compartment, it received an electric shock (1 mA, 3 s duration). Then the mouse was returned to its home cage. After 1 day, the mouse was placed in the illuminated compartment and the latency period to enter the dark compartment, defined as 'retention,' was measured. The time when the mouse entered the dark compartment was recorded and described as step-through latency. The retention trials were set at a limit of 180 s as cutoff time.

Brain tissue collection and preservation. After behavioral tests, animals were perfused with PBS under inhaled diethyl ether anesthetization. The brains were immediately removed from skull, and the cortex and hippocampus were dissected on ice. All the brain tissues were immediately stored at -80°C until biochemical assays were conducted.

Western blot analysis. Cells and each area of the brain tissue were homogenized and lysed by a 30 min incubation on ice. The lysates were centrifuged at 15 000 $\times$ r.p.m. for 15 min. An equal amount of total protein (20 μg) isolated from brain tissues was resolved on an sodium dodecyl sulfate (SDS) 10 or 12% polyacrylamide gel and then transferred to a nitrocellulose membrane (Hybond ECL; Amersham Pharmacia Biotech, Piscataway, NJ, USA). Blots were blocked for 1 h at room temperature with 5% (w/v) nonfat dried milk in Tris-buffered saline Tween-20 (TBST: 10 mM Tris (pH 8.0) and a 150 mM NaCl solution containing 0.05% Tween-20). After a short wash in TBST, membranes were incubated at 4°C with specific antibodies. The blot was then incubated with the HRP-conjugated anti-mouse or anti-rabbit antibodies (1 : 2000; Santa Cruz Biotechnology, Santa Cruz, CA, USA). Immunoreactive proteins were detected with the enhanced chemiluminescence (ECL) western blotting detection system.

Immunohistochemistry and immunofluorescence. Mice were anesthetized with ether. While under general anesthesia, the mice received intracardiac perfusion with 50 ml of saline. Brains were fixed in formalin and paraffin-enclosed for examination. Tissue sections, 5 μm thick, were used with immunohistochemistry (also used in immunofluorescence). Paraffin-embedded sections were deparaffinized and rehydrated, washed in distilled water, and then subjected to heat-mediated antigen retrieval treatment. Endogenous peroxidase activity was quenched by incubation in 1% hydrogen peroxide in methanol for 30 min and then cleared in PBS for 5 min. The sections were blocked for 30 min with 3% normal horse/goat serum diluted in PBS. These sections were incubated overnight with appropriate antibodies. After washing in PBS, the sections were incubated in biotinylated goat anti-mouse/rabbit IgG antibody (1 : 1000 dilution, Vector Laboratories, Burlingame, CA, USA) for 1 h at room temperature. The sections were subsequently washed and incubated with avidin-conjugated peroxidase complex (ABC kit, 1 : 200 dilution, Vector Laboratories) for 30 min followed by PBS washing. The peroxidase reaction was performed in PBS using 3, 3'-diaminobenzidine tetrahydrochloride (DAB, 0.02%) as the chromogen. Finally, sections were dehydrated in ethanol, cleared in xylene, and mounted with Permount (Fisher Scientific, Waltham, MA, USA), and evaluated on a light microscopy (Olympus, Tokyo, Japan). For immunofluorescence, sections were incubated with an anti-rabbit secondary antibody labeled with Alexa-Fluor 488 (1 : 400 dilution; Invitrogen, Carlsbad, CA, USA) or anti-mouse secondary antibody labeled with Alexa-Fluor 568 (1 : 400 dilution, Invitrogen) for 2 h at room temperature. Final images were acquired using a confocal laser scanning microscope (TCS SP2, Leica Microsystems AG, Werzlar, Germany).

Measurement of Aβ_{1-42}. Lysates of brain tissue were obtained through protein extraction buffer containing protease inhibitor. Aβ_{1-42} level was determined using each specific enzyme-linked immunosorbent assay (ELISA) Kit (Immuno-Biological Laboratories Co., Ltd, Takasaki-Shi, Gunma, Japan). In brief, 100 μl of sample was added into the precoated plate and was incubated overnight at 4°C. After washing each well of the precoated plate with washing buffer, 100 μl of labeled antibody solution was added and the mixture was incubated for 1 h at 4°C in the dark. After washing, chromogen was added and the mixture was incubated for 30 min at room temperature in the dark. Finally, the resulting color was assayed at 450 nm using a microplate absorbance reader (SunriseTM, TECAN, Switzerland) after adding stop solution.

TUNEL assay. DNA fragmentation was examined by terminal deoxynucleotidyl transferase-mediated FITC–dUDP nick-end labeling (TUNEL). TUNEL assays were performed using the *in situ* Cell Death Detection Kit (Roche Diagnostics GmbH, Mannheim, Germany) according to the manufacturer's instructions. Briefly, after fixation of 25-μm cryosections with 4% paraformaldehyde, treatment with 0.1% NaBH4 and 0.1 Triton X-100, the slides were incubated for at least 1 h with a reaction mix containing deoxynucleotidyl transferase and FITC–dUDP (Roche, Reinach, Switzerland). For 4′,6′-diamidino-2-phenylindole dihydrochloride (DAPI) staining, slides were incubated for 15 min at room temperature in the dark with mounting medium for fluorescence containing DAPI (Vector Laboratories). The tissues were then observed through a fluorescence microscope (Leica Microsystems AG, Wetzlar, Germany) and the nuclei were visualized by the DAPI staining.

Proteome profiler arrays. The brain tissues were excised and homogenized in PBS with protease inhibitor cocktail (Sigma-Aldrich, St. Louis, MO, USA) and Triton X-100 (final concentration 1%). The samples were frozen at -70°C, thawed, and centrifuged at 10 000 $\times$ *g* for 5 min to remove any cellular debris. Proteins (200 μg) collected from three samples per group were used for mouse cytokine array according to the protocol provided by supplier (Proteome Profiler, ARY006, R&D Systems).

Statistical analysis. The data were analyzed using the GraphPad Prism version 4 program (GraphPad Software, Inc., San Diego, CA, USA). Data are presented as mean $\pm$ S.D. Statistical significance was performed on the data

using one-way analysis of variance (ANOVA) or unpaired Student's *t*-test. A value of $P<0.05$ was considered to be statistically significant.

Conflict of Interest

The authors declare no conflict of interest.

Acknowledgements. This work was supported by a grant from the National Research Foundation of Korea (NRF) funded by the Korean Government (MRC 2008-0062275), by a grant (A101836) from the Korean Health Technology R&D Project, Ministry for Health, Welfare and Family Affairs, Republic of Korea and by the Priority Research Centres Program through the NRF funded by the Ministry of Education, Science and Technology (2009-0094034).

1. Momin EN, Mohyeldin A, Zaidi HA, Vela G, Quinones-Hinojosa A. Mesenchymal stem cells: new approaches for the treatment of neurological diseases. *Curr Stem Cell Res Ther* 2010; **5**: 326–344.
2. Peng Y, Huang S, Cheng B, Nie X, Enhe J, Feng C *et al.* Mesenchymal stem cells: a revolution in therapeutic strategies of age-related diseases. *Ageing Res Rev* 2013; **12**: 103–115.
3. Baksh D, Song L, Tuan RS. Adult mesenchymal stem cells: characterization, differentiation, and application in cell and gene therapy. *J Cell Mol Med* 2004; **8**: 301–316.
4. Friedenstein AJ, Chailakhjan RK, Lalykina KS. The development of fibroblast colonies in monolayer cultures of guinea-pig bone marrow and spleen cells. *Cell Tissue Kinet* 1970; **3**: 393–403.
5. Pittenger MF, Mackay AM, Beck SC, Jaiswal RK, Douglas R, Mosca JD *et al.* Multilineage potential of adult human mesenchymal stem cells. *Science* 1999; **284**: 143–147.
6. Stenderup K, Justesen J, Clausen C, Kassem M. Aging is associated with decreased maximal life span and accelerated senescence of bone marrow stromal cells. *Bone* 2003; **33**: 919–926.
7. Ringe J, Kaps C, Burmester GR, Sittinger M. Stem cells for regenerative medicine: advances in the engineering of tissues and organs. *Naturwissenschaften* 2002; **89**: 338–351.
8. Brooke G, Rossetti T, Pelekanos R, Ilic N, Murray P, Hancock S *et al.* Manufacturing of human placenta-derived mesenchymal stem cells for clinical trials. *Br J Haematol* 2009; **144**: 571–579.
9. Jones RJ, Matsui W. Cancer stem cells: from bench to bedside. *Biol Blood Marrow Transplant* 2007; **13**(Suppl 1): 47–52.
10. Barlow S, Brooke G, Chatterjee K, Price G, Pelekanos R, Rossetti T *et al.* Comparison of human placenta- and bone marrow-derived multipotent mesenchymal stem cells. *Stem Cells Dev* 2008; **17**: 1095–1107.
11. Tran TC, Kimura K, Nagano M, Yamashita T, Ohneda K, Sugimori H *et al.* Identification of human placenta-derived mesenchymal stem cells involved in re-endothelialization. *J Cell Physiol* 2011; **226**: 224–235.
12. Lee JK, Jin HK, Bae JS. Bone marrow-derived mesenchymal stem cells reduce brain amyloid-beta deposition and accelerate the activation of microglia in an acutely induced Alzheimer's disease mouse model. *Neurosci Lett* 2009; **450**: 136–141.
13. Lee JK, Jin HK, Bae JS. Bone marrow-derived mesenchymal stem cells attenuate amyloid beta-induced memory impairment and apoptosis by inhibiting neuronal cell death. *Curr Alzheimer Res* 2010; **7**: 540–548.
14. Lee JK, Jin HK, Endo S, Schuchman EH, Carter JE, Bae JS. Intracerebral transplantation of bone marrow-derived mesenchymal stem cells reduces amyloid-beta deposition and rescues memory deficits in Alzheimer's disease mice by modulation of immune responses. *Stem Cells* 2010; **28**: 329–343.
15. Lee HJ, Lee JK, Lee H, Carter JE, Chang JW, Oh W *et al.* Human umbilical cord blood-derived mesenchymal stem cells improve neuropathology and cognitive impairment in an Alzheimer's disease mouse model through modulation of neuroinflammation. *Neurobiol Aging* 2012; **33**: 588–602.
16. Selkoe DJ. Alzheimer's disease. In the beginning. *Nature* 1991; **354**: 432–433.
17. Craft S. The role of metabolic disorders in Alzheimer disease and vascular dementia: two roads converged. *Arch Neurol* 2009; **66**: 300–305.
18. Zetterberg H, Blennow K, Hanse E. Amyloid beta and APP as biomarkers for Alzheimer's disease. *Exp Gerontol* 2010; **45**: 23–29.
19. Lee YJ, Choi DY, Lee YK, Lee YM, Han SB, Kim YH *et al.* 4-O-methylhonokiol prevents memory impairment in the Tg2576 transgenic mice model of Alzheimer's disease via regulation of beta-secretase activity. *J Alzheimers Dis* 2012; **29**: 677–690.
20. LeBlanc AC, Papadopoulos M, Belair C, Chu W, Crosato M, Powell J *et al.* Processing of amyloid precursor protein in human primary neuron and astrocyte cultures. *J Neurochem* 1997; **68**: 1183–1190.
21. Fuller S, Munch G, Steele M. Activated astrocytes: a therapeutic target in Alzheimer's disease? *Expert Rev Neurother* 2009; **9**: 1585–1594.
22. Leung E, Guo L, Bu J, Maloof M, El Khoury J, Geula C. Microglia activation mediates fibrillar amyloid-beta toxicity in the aged primate cortex. *Neurobiol Aging* 2011; **32**: 387–397.
23. Zhao J, O'Connor T, Vassar R. The contribution of activated astrocytes to Abeta production: implications for Alzheimer's disease pathogenesis. *J Neuroinflammation* 2011; **8**: 150.
24. Schubert D, Soucek T, Blouw B. The induction of HIF-1 reduces astrocyte activation by amyloid beta peptide. *Eur J Neurosci* 2009; **29**: 1323–1334.
25. Rossner S, Lange-Dohna C, Zeitschel U, Perez-Polo JR. Alzheimer's disease beta-secretase BACE1 is not a neuron-specific enzyme. *J Neurochem* 2005; **92**: 226–234.
26. Nitta A, Itoh A, Hasegawa T, Nabeshima T. beta-Amyloid protein-induced Alzheimer's disease animal model. *Neurosci Lett* 1994; **170**: 63–66.
27. Tsukuda K, Mogi M, Iwanami J, Min LJ, Sakata A, Jing F *et al.* Cognitive deficit in amyloid-beta-injected mice was improved by pretreatment with a low dose of telmisartan partly because of peroxisome proliferator-activated receptor-gamma activation. *Hypertension* 2009; **54**: 782–787.
28. Burgos-Ramos E, Puebla-Jimenez L, Arilla-Ferreiro E. Minocycline provides protection against beta-amyloid(25–35)-induced alterations of the somatostatin signaling pathway in the rat temporal cortex. *Neuroscience* 2008; **154**: 1458–1466.
29. Kim TI, Lee YK, Park SG, Choi IS, Ban JO, Park HK *et al.* l-Theanine, an amino acid in green tea, attenuates beta-amyloid-induced cognitive dysfunction and neurotoxicity: reduction in oxidative damage and inactivation of ERK/p38 kinase and NF-kappaB pathways. *Free Radic Biol Med* 2009; **47**: 1601–1610.
30. Choi IS, Lee YJ, Choi DY, Lee YK, Lee YH, Kim KH *et al.* 4-O-methylhonokiol attenuated memory impairment through modulation of oxidative damage of enzymes involving amyloid-beta generation and accumulation in a mouse model of Alzheimer's disease. *J Alzheimers Dis* 2011; **27**: 127–141.
31. Lee YK, Choi IS, Ban JO, Lee HJ, Lee US, Han SB *et al.* 4-O-methylhonokiol attenuated beta-amyloid-induced memory impairment through reduction of oxidative damages via inactivation of p38 MAP kinase. *J Nutr Biochem* 2011; **22**: 476–486.
32. Choi DY, Lee JW, Peng J, Lee YJ, Han JY, Lee YH *et al.* Obovatol improves cognitive functions in animal models for Alzheimer's disease. *J Neurochem* 2012; **120**: 1048–1059.
33. Yun HM, Jin P, Han JY, Lee MS, Han SB, Oh KW *et al.* Acceleration of the development of Alzheimer's disease in amyloid beta-infused peroxiredoxin 6 overexpression transgenic mice. *Mol Neurobiol* 2013; **48**: 941–951.
34. Selkoe DJ. The molecular pathology of Alzheimer's disease. *Neuron* 1991; **6**: 487–498.
35. Hardy JA, Higgins GA. Alzheimer's disease: the amyloid cascade hypothesis. *Science* 1992; **256**: 184–185.
36. Park D, Yang G, Bae DK, Lee SH, Yang YH, Kyung J *et al.* Human adipose tissue-derived mesenchymal stem cells improve cognitive function and physical activity in ageing mice. *J Neurosci Res* 2013; **91**: 660–670.
37. Heneka MT, Sastre M, Dumitrescu-Ozimek L, Dewachter I, Walter J, Klockgether T *et al.* Focal glial activation coincides with increased BACE1 activation and precedes amyloid plaque deposition in APP[V717I] transgenic mice. *J Neuroinflammation* 2005; **2**: 22.
38. Yamamoto M, Kiyota T, Horiba M, Buescher JL, Walsh SM, Gendelman HE *et al.* Interferon-gamma and tumor necrosis factor-alpha regulate amyloid-beta plaque deposition and beta-secretase expression in Swedish mutant APP transgenic mice. *Am J Pathol* 2007; **170**: 680–692.
39. Bourne KZ, Ferrari DC, Lange-Dohna C, Rossner S, Wood TG, Perez-Polo JR. Differential regulation of BACE1 promoter activity by nuclear factor-kappaB in neurons and glia upon exposure to beta-amyloid peptides. *J Neurosci Res* 2007; **85**: 1194–1204.
40. Jin P, Kim JA, Choi DY, Lee YJ, Jung HS, Hong JT. Anti-inflammatory and anti-amyloidogenic effects of a small molecule, 2,4-bis(p-hydroxyphenyl)-2-butenal in Tg2576 Alzheimer's disease mice model. *J Neuroinflammation* 2013; **10**: 2.
41. Ponomarev ED, Maresz K, Tan Y, Dittel BN. CNS-derived interleukin-4 is essential for the regulation of autoimmune inflammation and induces a state of alternative activation in microglial cells. *J Neurosci* 2007; **27**: 10714–10721.
42. Clausen BH, Lambertsen KL, Babcock AA, Holm TH, Dagnaes-Hansen F, Finsen B. Interleukin-1beta and tumor necrosis factor-alpha are expressed by different subsets of microglia and macrophages after ischemic stroke in mice. *J Neuroinflammation* 2008; **5**: 46.
43. Halle A, Hornung V, Petzold GC, Stewart CR, Monks BG, Reinheckel T *et al.* The NALP3 inflammasome is involved in the innate immune response to amyloid-beta. *Nat Immunol* 2008; **9**: 857–865.
44. Wyss-Coray T. Inflammation in Alzheimer disease: driving force, bystander or beneficial response? *Nat Med* 2006; **12**: 1005–1015.
45. Mehlhorn G, Hollborn M, Schliebs R. Induction of cytokines in glial cells surrounding cortical beta-amyloid plaques in transgenic Tg2576 mice with Alzheimer pathology. *Int J Dev Neurosci* 2000; **18**: 423–431.
46. Tuppo EE, Arias HR. The role of inflammation in Alzheimer's disease. *Int J Biochem Cell Biol* 2005; **37**: 289–305.
47. Jana A, Pahan K. Fibrillar amyloid-beta-activated human astroglia kill primary human neurons via neutral sphingomyelinase: implications for Alzheimer's disease. *J Neurosci* 2010; **30**: 12676–12689.
48. Wallach D. Cell death induction by TNF: a matter of self control. *Trends Biochem Sci* 1997; **22**: 107–109.

49. Xia MQ, Bacskai BJ, Knowles RB, Qin SX, Hyman BT. Expression of the chemokine receptor CXCR3 on neurons and the elevated expression of its ligand IP-10 in reactive astrocytes: in vitro ERK1/2 activation and role in Alzheimer's disease. *J Neuroimmunol* 2000; **108**: 227–235.
50. Garwood CJ, Pooler AM, Atherton J, Hanger DP, Noble W. Astrocytes are important mediators of Abeta-induced neurotoxicity and tau phosphorylation in primary culture. *Cell Death Dis* 2011; **2**: e167.
51. Tang YL, Zhao Q, Qin X, Shen L, Cheng L, Ge J *et al.* Paracrine action enhances the effects of autologous mesenchymal stem cell transplantation on vascular regeneration in rat model of myocardial infarction. *Ann Thorac Surg* 2005; **80**: 229–236.
52. Beyer Nardi N, da Silva Meirelles L. Mesenchymal stem cells: isolation, in vitro expansion and characterization. *Handb Exp Pharmacol* 2006; **174**: 249–282.
53. Monje ML, Toda H, Palmer TD. Inflammatory blockade restores adult hippocampal neurogenesis. *Science* 2003; **302**: 1760–1765.
54. Zhao C, Deng W, Gage FH. Mechanisms and functional implications of adult neurogenesis. *Cell* 2008; **132**: 645–660.
55. Bellucci A, Luccarini I, Scali C, Prosperi C, Giovannini MG, Pepeu G *et al.* Cholinergic dysfunction, neuronal damage and axonal loss in TgCRND8 mice. *Neurobiol Dis* 2006; **23**: 260–272.
56. Nakatsu SL, Masek MA, Landrum S, Frenster JH. Activity of DNA templates during cell division and cell differentiation. *Nature* 1974; **248**: 334–335.
57. Taupin P. Adult neurogenesis in mammals. *Curr Opin Mol Ther* 2006; **8**: 345–351.
58. Hastings NB, Gould E. Rapid extension of axons into the CA3 region by adult-generated granule cells. *J Comp Neurol* 1999; **413**: 146–154.
59. Zhao C, Teng EM, Summers RG Jr, Ming GL, Gage FH. Distinct morphological stages of dentate granule neuron maturation in the adult mouse hippocampus. *J Neurosci* 2006; **26**: 3–11.
60. Jang MJ, Kim HS, Lee HG, Kim GJ, Jeon HG, Shin HS *et al.* Placenta-derived mesenchymal stem cells have an immunomodulatory effect that can control acute graft-versus-host disease in mice. *Acta Haematol* 2012; **129**: 197–206.

Supplementary Information accompanies this paper on Cell Death and Disease website (http://www.nature.com/cddis)